Electronic Structure of CO—An Exercise in Modern Chemical Bonding Theory

GERNOT FRENKING,[1] CHRISTOPH LOSCHEN,[1] ANDREAS KRAPP,[1] STEFAN FAU,[1] STEVEN H. STRAUSS[2]

[1]*Fachbereich Chemie, Philipps-Universität Marburg, Marburg D-35032, Germany*
[2]*Department of Chemistry, Colorado State University, Fort Collins, Colorado 80523*

Abstract: This paper discusses recent progress that has been made in the understanding of the electronic structure and bonding situation of carbon monoxide which was analyzed using modern quantum chemical methods. The new results are compared with standard models of chemical bonding. The electronic charge distribution and the dipole moment, the nature of the HOMO and the bond dissociation energy are discussed in detail.

© 2006 Wiley Periodicals, Inc.   J Comput Chem 28: 117–126, 2007

Key words: carbon monoxide; bonding analysis; dipole moment

Introduction

Describing the electronic structure of, and the nature of the bond in, carbon monoxide in terms of simple bonding models is not a trivial task because of the unusual chemical and physical properties of the molecule, the only monocoordinated carbon compound that is stable under normal conditions. It has been called "an isolated embarrassment for introductory chemistry teachers,"[1] and it exhibits several surprising features: (i) the triple bond between the atoms is a very unusual atomic valence state for both atoms but particularly for oxygen; there is also a mismatch between the formal oxidation states of the atoms ($+2$ for carbon and -2 for oxygen) and the triple bond; (ii) the dipole moment of the molecule is small (0.11 D)[2] with the negative end at the carbon atom although carbon is clearly less electronegative than oxygen; (iii) the bond dissociation energy (BDE) of CO (255.7 kcal/mol) is significantly higher than that of isoelectronic N_2 (225.1 kcal/mol)[3]; (iv) the carbon–oxygen bond in CO becomes stronger when the carbon atom forms a σ bond with another atom but becomes weaker when the oxygen atom forms a σ bond with another atom.

Modern textbooks of general and inorganic chemistry generally offer the standard explanations (*vide infra*) for findings (i)–(iv) if they are explained at all. However, the bonding properties of CO as ligand in transition metal (TM) chemistry, where carbonyl complexes are a ubiquitous class of compounds, have recently been the focus of extensive experimental and theoretical studies which have shed new light on the chemical behavior of this important molecule.[4–8] The new findings challenge some of the standard textbook explanations. Also, the nature of the chemical bond in CO and the reason why its BDE is larger than that of N_2 have recently been reinvestigated (the details of the calculations are given in ref. 9). It thus seems appropriate to review the

recent quantum-chemical investigations of the chemical bonding in CO which help to build a bridge between the physical properties of CO and the heuristic bonding models which are used as pedagogical tools in chemistry courses and textbooks.

Electronic Structure, Charge Distribution, Dipole Moment, and Chemical Reactivity

A very useful starting point for a discussion of the electronic structure of CO is the electron density distribution $\rho(r)$ which gives important information about the topography of the electronic charge in the molecule. Pioneering studies by Bader[10] have shown that essential features of the electronic structure are nicely revealed when the second derivative of the charge distribution $\nabla^2\rho(r)$, which is called the Laplacian distribution, is used for the analysis of the bonding situation. The Laplacian distribution indicates local areas where the electron density is concentrated ($\nabla^2\rho(r) < 0$) and areas where the charge is depleted ($\nabla^2\rho(r) > 0$). Figure 1 shows the Laplacian distribution of CO which was calculated at the B3LYP/6-31G(d) level.

It becomes obvious that the topography of the electronic charge distribution at the carbon atom is very different from that of the oxygen atom. The contour line diagram of $\nabla^2\rho(r)$ indicates that the electronic charge at the latter atom has a spherical shape in the three-dimensional space, while the carbon atom has a rather anisotropical charge distribution. In particular, there is a droplet-like

Correspondence to: G. Frenking; e-mail: frenking@chemie.uni-marburg.de
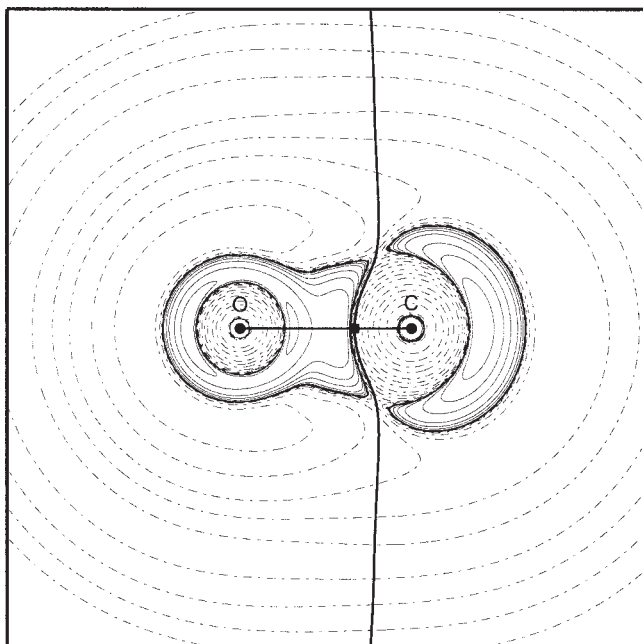
Figure 1. Laplacian distribution of CO. Solid lines indicate areas of charge concentration ($\bigtriangledown^2\rho(r) < 0$) while dashed lines show areas of charge depletion ($\bigtriangledown^2\rho(r) > 0$).

appendix of charge concentration ($\bigtriangledown^2\rho(r) < 0$, solid lines) at the carbon atom pointing away from the oxygen atom which can be identified with σ charge, i.e. it comes from orbitals having σ symmetry. In contrast to this, there are areas of charge depletion ($\bigtriangledown^2\rho(r) > 0$, dashed lines) at carbon in a direction which is orthogonal to the C—O bond path. The latter can be identified with a "hole" in the π charge-distribution at the carbon atom. It is tempting to correlate the shape of the Laplacian distribution of CO with its chemical behavior, i.e. carbon monoxide being a σ base and a π acid. This judgement would be rash, however, because the chemical reactivity of a molecule is mainly determined by its valence electrons and less by the total electron density distribution. In particular, the electrons in the frontier orbital(s) play a special role for the chemical reactivity.[11] In CO, the charge concentration at carbon coincides with the spatial extension of the HOMO which is mainly a lone pair orbital at carbon (see below) while the π* LUMO coincides with the area of charge depletion. However, there are cases where the shapes of the frontier orbitals do not agree with the topography of the charge distribution.

The topography of the total electron density distribution determines the dipole moment of a molecule. The Laplacian distribution shown in Figure 1 illustrates nicely why the negative end of the dipole moment of CO is at the carbon atom. The area of electronic charge concentration ($\bigtriangledown^2\rho(r) < 0$) at the carbon atom is rather far away from the nucleus which yields a significant component of the total dipole moment. The area of charge concentration at oxygen is much closer to the nucleus which induces a smaller dipole component towards the oxygen end. We want to point out that the dipole moment is determined by the charge distribution $\rho(r)$ and not by the Laplacian distribution $\bigtriangledown^2\rho(r)$. The distribution of $\bigtriangledown^2\rho(r)$ is a sensitive probe, however, for the ani-

sotropy of $\rho(r)$ which therefore helps to understand how the charge distribution yields a dipole moment.

It is important to realize that the dipole moment is a vector quantity, not a scalar quantity. This means that the shape of the electronic charge distribution may be more important for the dipole moment than the size of the atomic charge. The thick line in Figure 1 which crosses the C—O bond path at the bond critical point separates the atoms in the molecule in a mathematically well defined way.* The line denotes the so called zero-flux surface which defines the atomic basins of C and O. Integration of the electronic charge over the atomic basins give the total atomic charges of CO. The calculation gives rather large atomic charges where the carbon atom is positively charged with $q(C) = +1.33$e. Other charge partitioning methods give smaller absolute values but they all agree that the carbon atom in CO carries a positive partial charge. It is misleading to use the atomic partial charge q as an indicator of the dipole moment because q is a scalar quantity which has no information about the topography of the charge distribution. Since the topography of the electronic charge distribution is also very important for the chemical reactivity, caution should be employed when the atomic charges are used for an interpretation of chemical reactivity.

Further insight into the electronic structure of CO can be obtained when the molecular orbitals of the molecule are analyzed. Figure 2 shows the occupied core and valence MOs of carbon monoxide. Table 1 gives the calculated dipole moment contributions of each MO. They have been obtained by freezing the orbital coefficients of the respective occupied MO, deleting the other MOs and then calculating the remaining CO^{12+} species. The sum of the orbital components gives the total dipole moment $\mu = 0.18$ D which is in very good agreement with the experimental value $\mu = 0.11$ D.[2] Note that the calculation gives the right direction of the dipole moment, i.e. the positive value indicates that the carbon atom carries its negative end. The 1σ and 2σ core orbitals have large dipole moments because the electrons are localized at the oxygen and carbon atom, respectively. All valence orbitals except the 7σ HOMO have negative dipole moments which means that the electronic charge is distorted in such a way that the negative end of the dipole moment is at the oxygen atom. Without the HOMO the calculated dipole moment of CO would be $\mu = -8.03$ D. The calculations demonstrate nicely that it is the very strong dipole moment component of the lone-pair HOMO ($\mu = 8.21$ D) which shifts the total dipole moment of CO towards having the negative end at the carbon atom. Inspection of the shape of the 7σ HOMO shows a large area of charge concentration at the carbon atom pointing away from oxygen.

The topography of the electronic charge concentration of a molecule determines not only its dipole moment, it is also relevant for its chemical reactivity. It is known from frontier orbital theory[11] that the energy level and the shape of the frontier orbitals

---

*At a bond critical point the first derivative of the electronic charge $\bigtriangledown\rho(r)$ is zero, while the second derivative $\bigtriangledown^2\rho(r)$ along the internuclear axis is positive and the values of the other two second derivatives in the plane which is perpendicular to the internuclear axis are negative, i.e. ρ is a minimum in one direction and a maximum in the other two directions. For further details see ref. 9.
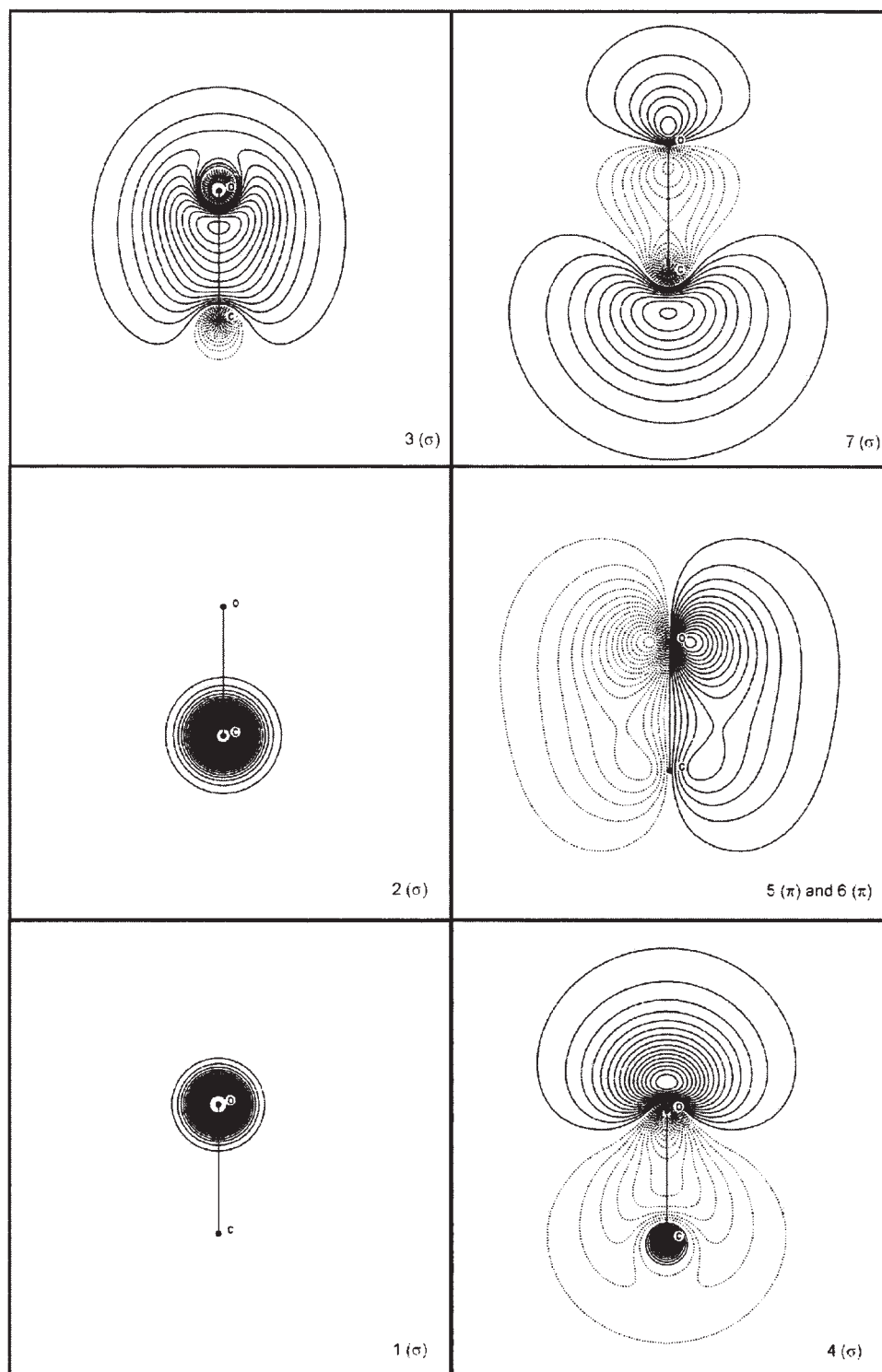
Figure 2. Occupied core (1,2) and valence (3,7) molecular orbitals of CO.

determine how a molecule reacts in orbital-controlled reactions and how it may bind to other atoms or molecules. The arguments given above suggest that CO should react with electrophilic reagents as a nucleophilic agent through its σ-donor orbital and that it should preferentially bind through its 7σ HOMO to electron-deficient species. There is ubiquitous experimental evidence for this. However, this behavior can only be understood when the topographical property of the electron density distribution of CO is

Table 1. Orbital Components to the Total Dipole Moment of CO at BP86/6-311++G(3df, 3pd).[a]

Orbital	Bond moment
MO 1 σ	−4.67
MO 2 σ	6.23
MO 3 σ	−1.57
MO 4 σ	−4.52
MO 5 π	−1.75
MO 6 π	−1.75
MO 7 σ (HOMO)	8.21
Σ	*0.18 (exp. 0.11)*

[a]Values in Debye. Positive values indicate that the negative end is at the carbon atom. The origin of the CO^{12+} ion is chosen at the position where the dipole moment of the nuclei becomes zero. The orbital components were calculated with nuclear charges which are scaled by 6/7 (carbon) and 8/7 (oxygen). This leads to orbital components of the dipole which after summation give the total dipole moment of the neutral molecule which is origin independent.

considered but not the atomic partial charge. Otherwise, the reactivity and bonding property of carbon monoxide can be misinterpreted. A very common mistake which is found in the literature is to equate atomic partial charges with nucleophilic or electrophilic behavior of that atom in a molecule. For example, it was claimed that the carbon atom of CO in the positively charged hexacarbonyls $[Os(CO)_6]^{2+}$ and $[Ir(CO)_6]^{3+}$ is electrophilic rather than nucleophilic because the calculated atomic partial charge of carbon is more positive than that of the metals.[5,12] The authors failed to recognize the pivotal influence of the topography of the electronic charge distribution.

Is the 7σ HOMO of CO Bonding or Antibonding?

The chemical bonding of CO in TM carbonyl complexes is usually described in terms of the Dewar–Chatt–Duncanson bonding model which suggests synergistic donation from the 7σ HOMO of CO into an empty σ orbital of the metal and backdonation from an occupied d(π) orbital of the metal into the empty π^* orbital of CO (see Fig. 3).[13] Numerous theoretical studies support the bonding model.[8,14]

The C—O stretching frequencies of most metal carbonyls are shifted to lower wavenumbers relative to free CO. This can be explained with the M(π)→CO(π^*) backdonation which weakens the C—O bond. The M(σ^*)←CO(σ) donation has less influence on the C—O stretching mode.[15] However, there is a class of metal carbonyls called "nonclassical" which have C—O stretching frequencies that are shifted to higher wavenumbers compared with free CO.[4] Nonclassical behavior is found when the metal atom carries a positive charge which diminishes the M(π)→ CO(π^*) backdonation. Thus, the shift to higher stretching frequencies in nonclassical carbonyls might be explained in terms of M(σ^*)←CO(σ) donation. A simple molecule where only σ-bonding with CO is possible is the formyl cation HCO^+ which has a C—O stretching frequency that is significantly higher (2245 cm^{-1})

than in free CO (2143 cm^{-1}). The larger wave number suggests that C—O bonding in HCO^+ is stronger than in free CO which is in agreement with the shorter C—O bond length in the former molecule (1.1047 Å) than in the latter (1.1283 Å).[3,16] The cation CO^+ has also a higher stretching mode (2214 cm^{-1}) and a shorter bond (1.1151 Å) than CO.[3] Why does σ charge donation from CO shorten the bond and increase the frequency of the stretching mode?

A straightforward explanation would be that the 7σ HOMO is antibonding. Removal of electronic charge from an antibonding orbital should yield stronger bonding which would explain the observed shift of the C—O stretching mode in σ-only bonded CO. Indeed, this explanation is used in textbooks[17] and in the recent literature.[7c] Visual inspection of the shape of the 7σ HOMO does not support the notion of an antibonding character, however. Figure 2 shows that there is no node between the oxygen and carbon atom in the orbital. To analyze the overall contributions of the 2s and 2p(σ) AOs of carbon and oxygen to the σ orbitals we calculated the size of their overlap integral values at different distances r_{C-O}. A graphical display of the plotted values are shown in Figure 4.

It becomes obvious that, at the equilibrium distance, the maximum value of the overlap of the σ orbitals has not yet been reached. The value for the total σ overlap (1.51) is the sum of the contributions from the overlaps of the s-s (0.43), s-p_z (0.51 and 0.40), and p_z-p_z (0.17) orbitals where z is the molecular axis. The latter value is rather small because the p_z orbitals are partially overlapping in the antibonding area, but the overlap is still positive. Note that the value of the π overlap ($2 \times 0.35 = 0.70$) is less than half of the σ overlap (1.51).

Where does the statement about the antibonding nature of the 7σ HOMO come from? It is interesting to examine the reasonings which are given in the literature. In the textbook *Orbital Interactions in Chemistry* by Albright, Burdett, and Whangbo it is shown[17a] that the 7σ HOMO of CO can not reliably be constructed from the atomic orbitals using perturbation theory because the energy levels of the 2s AO of carbon and the 2s AO of oxygen are nearly degenerate. The orbital can only be calculated using variational principles. The authors then say that the antibonding nature of the 7σ HOMO of CO becomes obvious through the shift of the C—O stretching frequency towards lower wavenumbers when one electron is removed from the orbital yielding the radical cation CO^+. However, the argumentation does not consider alternative explanations for the frequency shift which are in agreement with the shape of the 7σ HOMO of CO.

A theoretically better founded reasoning for the stated antibonding nature is given in the recent literature where the Mulliken
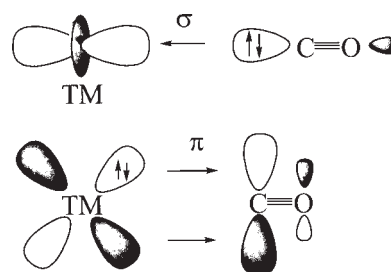
Figure 3. Schematic representation of the Dewar–Chatt–Duncanson donor–acceptor bonding model for CO.
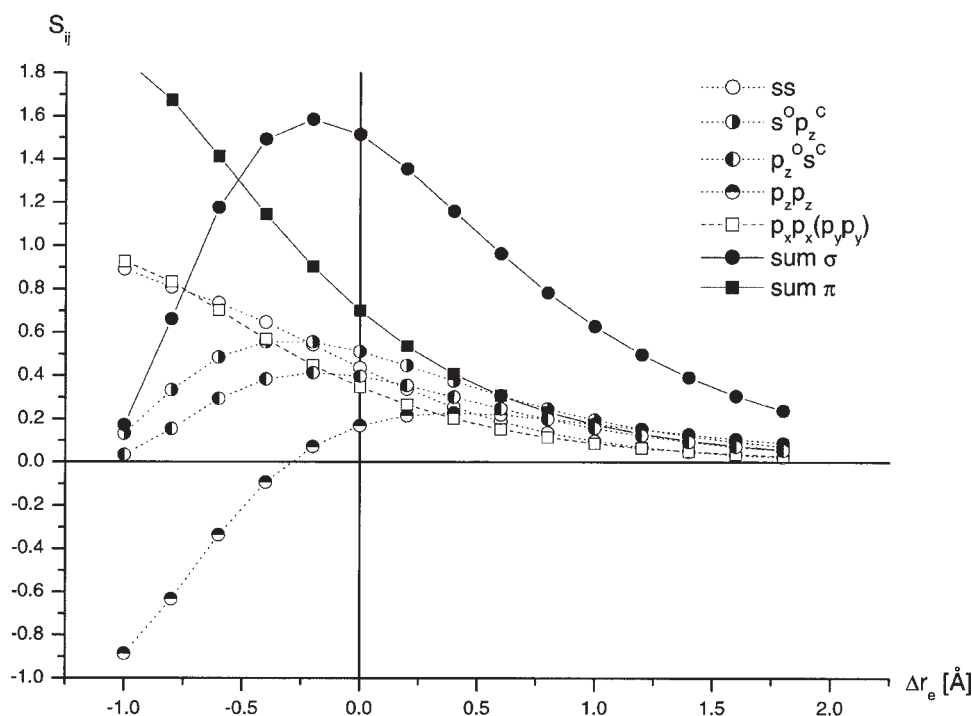
Figure 4. Plot of the overlap integrals S_{ij} of the 2s and 2p valence AOs of carbon and CO at different interatomic distances r_{C-O}. The reference value of Δr_e at 0.0 is the equilibrium distance.

overlap population of the orbital is used which has a negative value for the 7σ HOMO.[7c] However, the authors report in the same publication that the 7σ HOMO of N_2 has also a negative overlap population. The N—N bond length of N_2^+ (1.116 Å) is longer than in free N_2 (1.098 Å) and the stretching mode in the cation (2207 cm^{-1}) is shifted to lower wavenumber compared with dinitrogen (2359 cm^{-1}) which does not agree with an anti-bonding nature of the HOMO.[2]

A strong argument against an antibonding nature of the 7σ HOMO of CO comes from theoretical studies which investigate the change of the C—O distance when a proton H$^+$ or a positive point charge Q$^+$, which does not have an empty orbital, approaches the molecule from the carbon or from the oxygen end.[6] Figure 5 displays the change of the C—O bond lengths for the different approaches.

Two points are noteworthy when Figure 5 is examined. (a) The C—O interatomic distances decreases when H$^+$ or Q$^+$ approach the carbon atom of CO but the bond length increases when they approach from the oxygen end. (b) At the equilibrium distances, the C—O bond shortenings in HCO$^+$ and QCO$^+$ are nearly identical and also the C—O bond lengthenings in COH$^+$ and COQ$^+$ are essentially the same. The latter finding shows that the change in the C—O bond length is not caused by any charge donation from CO to H$^+$ but rather by an inductive charge effect.

An explanation for the above findings is given by comparison of the calculated polarization of the C—O valence orbitals in free CO with those in HCO$^+$, QCO$^+$, COH$^+$, and COQ$^+$. To facilitate the comparison we use the natural bond orbitals (NBO) of the molecule which show for CO the familiar picture of a σ-bonding and

degenerate π-bonding MO besides lone-pair orbitals at carbon and oxygen. The NBO picture thus supports the Lewis structure $(-)|C\equiv O|(+)$ for CO which obeys the octet rule. Table 2 shows that the σ-bonding MO (relative weight carbon to oxygen 27:73) and the degenerate π-bonding MO (24:76) are as expected strongly localized toward the oxygen atom because oxygen is more electro-negative than carbon. The polarization becomes less in HCO$^+$ and QCO$^+$ because the positively charged species attracts electronic charge from CO. The opposite effect is found in COH$^+$ and COQ$^+$. Here the polarization towards oxygen increases because electronic charge is further shifted due to the positively charged species which is bonded to oxygen. Figure 5 and Table 2 show that this is a purely electrostatic effect which has nothing to do with the formation of a σ bond H—CO$^+$ and CO—H$^+$ because the same effect is caused by the orbital-free species Q$^+$. The top of Figure 5 shows a qualitative illustration of the effect which leads to a C—O bond shortening in HCO$^+$ and QCO$^+$ and a bond lengthening in COH$^+$ and COQ$^+$. Note that the sketch on top of Figure 5 illustrates the polarization of the π orbital. Table 2 shows that the same polarization is found for the σ orbitals. The electrostatic effect enhances the bonding overlap in the former species and re-duces it in the latter. The increase in the C—O stretching frequency in σ-bonded species XCO with electron-deficient species X is caused by the change in the polarization of the C—O bond-ing orbitals. The 7σ HOMO is a weakly bonding orbital whose bonding character is enhanced by the change of the polarization in HCO$^+$ and QCO$^+$.

The arguments given above suggest that the C—O bonding in HCO$^+$ and QCO$^+$ becomes more like in N_2 which has a nonpolar
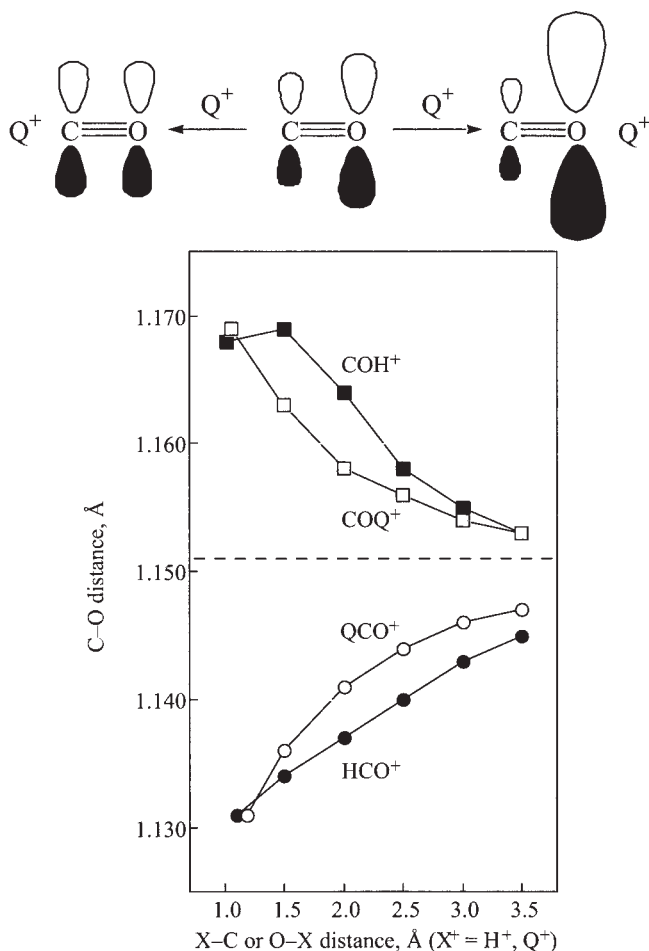
Figure 5. (Top) Effect of a positive charge on the polarization of the π HOMO of CO. The same effect is found for the σ-bonding orbital of CO. (Bottom) Plots of calculated distances for HCO^+, QCO^+, COH^+, and COQ^+ (Q^+ is a unit point charge; all species were constrained to be linear). The leftmost point for each species represents the equilibrium geometry. The dashed line at 1.151 Å represents the C—O distance in free CO at this level of theory. All calculations were done at MP2/6-31G(d). The data are from ref. 6b.

bond with maximum overlap of the σ and π overlap. Dinitrogen has indeed a shorter bond (1.0977 Å) than CO (1.1283 Å).[3] It has also a larger overlap of the σ (1.58) and π (0.74) orbitals than carbon monoxide, but it was said already that the BDE of N_2 is smaller than the BDE of CO. The reason for this will be discussed in the next section. Here we want to point out that the shorter C—O bond and the higher stretching frequency of HCO^+ compared with CO does not mean that the C—O bond energy of the former molecule is higher than that of the latter. Indeed, the experimental value for the BDE of HCO^+ yielding CH^+ + O is $D_o = 250.1$ kcal/mol which is less than the BDE of CO (255.7 kcal/mol).[18] (The BDE of HCO^+ was calculated from the experimental values for the heats of formation: $\Delta H_f^0(HCO^+) = 197.3$ kcal/mol; $\Delta H_f^0(CH^+) = 387.8$ kcal/mol; $\Delta H_f^0(O) = 59.6$ kcal/mol.[18])

The Nature of the Bonding in CO and a Comparison with Isoelectronic N_2 and BF

The nature of the chemical bonding in CO is usually considered in terms of covalent interactions, which consists of a σ bond and a degenerate π bond which are polarized towards the more electronegative oxygen atom. Since the orbital overlap in heteroatomic CO is smaller than in homoatomic N_2, it follows that the covalent attraction in CO should be weaker than in dinitrogen. However, carbon monoxide has a significantly stronger bond ($D_o = 255.7$ kcal/mol) than dinitrogen ($D_o = 225.1$ kcal/mol).[3] The standard textbook explanation for the stronger bond of CO goes back to Pauling[19] who suggested that heteroatomic covalent bonds are additionally stabilized by ionic contributions which in case of CO were estimated to be ~48 kcal/mol.[20] Without the ionic contribution, the chemical bonding in CO would be weaker than in N_2. But if this argument is true, why is it that the more polarized bond in isoelectronic BF is weaker than those of N_2 and CO?

There is an energy decomposition analysis (EDA) available which helps to address the above question.[21] According to the EDA method, the BDE ΔE (which is equal to $-D_e$ using the conventional term) between two atoms or fragments A and B is partitioned into several contributions which can be identified as physically meaningful entities. First, ΔE is separated into two major components ΔE_{prep} and ΔE_{int}:

$$\Delta E = \Delta E_{prep} + \Delta E_{int} \qquad (1)$$

ΔE_{prep} is the energy which is necessary to promote the fragments A and B from their equilibrium geometry and electronic ground state to the geometry and electronic state which they have in the compound AB. Since the fragments of CO are carbon and oxygen atoms in the triplet ground states, ΔE_{prep} is zero in our case. ΔE_{int} is the instantaneous interaction energy between the two fragments in the molecule. The latter quantity is the focus of the bonding analysis. The interaction energy ΔE_{int} is divided into three main components:

$$\Delta E_{int} = \Delta E_{elstat} + \Delta E_{Pauli} + \Delta E_{orb} \qquad (2)$$

ΔE_{elstat} gives the classical electrostatic interaction energy between the fragments which are calculated with a frozen electron density distribution in the geometry of the complex. ΔE_{Pauli} gives the repulsive interactions between the fragments which are caused by the fact that two electrons with the same spin can not occupy the same region in space. The term comprises the four electron destabilizing interactions between occupied orbitals. The stabilizing orbital interaction term ΔE_{orb} which can be identified with covalent bonding is calculated in the final step of the bonding analysis when the orbitals relax to their final form, i.e. when the occupied and the vacant orbitals of the fragments mix. The latter term can be further partitioned into contributions by orbitals which belong to different irreducible representations of the point group of the interacting system. In case of CO the ΔE_{orb} term can be partitioned into contributions of σ and π orbitals. Further details about the method have been described in the recent literature.[22] Reviews with a discussion of EDA results of chemical bonds have also recently been published.[23]

Table 2. NBO Localized Orbital Analysis of the Valence Orbitals of CO at MP2/6-31G(d).[a]

Molecule[b]	Bond AB	Occ[c]	Polar. A:B	Hybr(C)[d]	Hybr(O)[d]
CO	$CO(\sigma)$	1.98	27:73	24:75:0.5	44:55:0.7
	$CO(\pi)$ (2x)	1.95	24:76	0:99:0.7	0:100:0.4
	C(LP)	1.97		78:22:0.0	
	O(LP)	1.98			56:44:0.1
HCO^+	$CO(\sigma)$	1.98	32:68	42:58:0.2	40:60:0.6
	$CO(\pi)$ (2x)	1.94	30:70	0:100:0.5	0:100:0.5
	$HC(\sigma)$	1.98	33:67	59:41:0.1	
	O(LP)	1.98			60:40:0.1
QCO^+	$CO(\sigma)$	1.98	31:69	39:61:0.3	42:57:0.7
	$CO(\pi)$ (2x)	1.94	30:70	0:100:0.4	0:100:0.5
	C(LP)	1.98		60:40:0.2	
	O(LP)	1.98			58:42:0.1
COH^+	$CO(\sigma)$	1.98	22:78	20:80:0.7	55:45:0.3
	$CO(\pi)$ (2x)	1.96	15:85	0:99:1.2	0:100:0.1
	C(LP)	1.97		82:18:0.0	
	$OH(\sigma)$	1.98	86:14		45:55:0.1
COQ^+	$CO(\sigma)$	1.98	23:77	21:79:0.7	53:47:0.3
	$CO(\pi)$ (2x)	1.96	16:84	0:99:1.1	0:100:0.1
	C(LP)	1.97		82:18:0.0	
	O(LP)	1.98			46:54:0.2

[a]Data are taken from ref. 6b.
[b]QCO^+ and COQ^+ mean that a positive point charge Q^+ is attached to the carbon or oxygen end at the equilibrium distance.
[c]Occupation of the localized NBO orbital.
[d]Hybridization in % s, p, and d character of the hybrid orbitals; all delocalizations to other atoms are below 0.6%.

Please note that the electrostatic interaction energy ΔE_{elstat} must not be identified with ionic bonding. While purely ionic bonding in ionic crystals can be described in terms of classical electrostatic interactions, nonpolar bonds have usually also large contributions from classical electrostatic attraction. In 1986, Spackman and Maslen calculated the strength of the classical electrostatic interaction ΔE_{elstat} in 144 diatomic homoatomic and heteroatomic molecules.[24] They found that, in 143 molecules, electrostatic attraction is very strong and that ΔE_{elstat} may sometimes be larger than the BDE. The only diatomic molecule where ΔE_{elstat} was found to be very small is H_2. It is a myth that classical electrostatic attraction between the interpenetrating charges of neutral atoms which are bonded by a nonpolar bond is weak or even absent.

Table 3 gives the EDA results for N_2, CO, and BF using gradient corrected DFT at the RPBE/TZP level of theory.[9] For didactical purposes we discuss first the results for dinitrogen which have been obtained by calculating the interaction energies between the nitrogen atoms in the ^4S ground state (Fig. 6a). The total interaction energy is $\Delta E_{int} = -232.2$ kcal/mol which, after adding the zero-point energy contributions, gives a calculated BDE $D_o = 228.8$ kcal/mol that is in very good agreement with the experimental value $D_o = 225.0$ kcal/mol. The classical electrostatic contribution to the nitrogen–nitrogen bonding in N_2 is $\Delta E_{elstat} = -308.5$ kcal/mol, which is even bigger than the BDE. The covalent contributions to the bonding $\Delta E_{orb} = -715.4$ kcal/mol are very large but the Pauli repulsion $\Delta E_{Pauli} = 791.7$ kcal/mol is even larger. If electrostatic interactions would be ruled only by classical laws the chemical bond in N_2 would be much shorter than it really

is.[25] (In ref. 23 it is shown that N_2 would have an equilibrium distance of ~0.85 Å if the interatomic forces would obey classical laws of electrostatic forces. A further discussion of this is also given in ref. 25.) The EDA results indicate that the covalent bonding in N_2 comes from 65.7% σ bonding and 34.3% π bonding.

The arrangement of the oxygen and carbon atoms in their electronic ground state (^3P) yielding CO is not as clear as for N_2. Figures 6b and 6c show two possibilities. The orientation of the atoms which is given in Figure 6b agrees with the symmetry-allowed dissociation path since the electronic structure of carbon and oxygen atom has $C_{\infty v}$ symmetry with respect to the molecular axis. This means that the C–O σ bond comes from donor–acceptor interactions while the degenerate π bond comes from electron-sharing interactions. Figure 6c shows another arrangement where the electronic structure has only C_{2v} symmetry. The latter model for the bond formation has electron-sharing interactions for the σ bond while the two components of the π bond consist of one donor–acceptor bond and one electron-sharing bond. Although the latter arrangement does not agree with the overall symmetry along the bond formation pathway we also carried out EDA calculations for the C_{2v} approach.

The calculations give a higher BDE for CO $D_o = 255.4$ kcal/mol which is in excellent agreement with the experimental value $D_o = 255.7$ kcal/mol. What does the EDA say about the reason for the stronger bond than in N_2? We first discuss the EDA results for the $C_{\infty v}$ arrangement of the atomic electronic structures (Fig. 6b). Table 3 shows that the classical electrostatic attraction in CO is $\Delta E_{elstat} = -240.0$ kcal/mol which is much less than in N_2! The ex-

Table 3. Energy Partitioning Analysis of the N—N, C—O, and B—F Bonds at RPBE/TZP.[a]

	N$_2$	CO	CO	BF
Symmetry[b]	D$_{\infty h}$	C$_{\infty v}$	C$_{2v}$	C$_{\infty v}$
ΔE_{int}	−232.2	−258.4	−258.4	−180.8
ΔE_{Pauli}	791.7	575.8	725.9	476.1
ΔE_{Elstat}[c]	−308.5 (30.1)	−240.0 (28.8)	−291.1 (29.6)	−210.5 (32.0)
ΔE_{Orb}[c]	−715.4 (69.9)	−594.2 (71.2)	−693.2 (70.4)	−446.4 (68.0)
ΔE_{σ}[d]	−470.0 (65.7)	−301.7 (50.8)	−464.7 (67.0)	−396.4 (88.8)
ΔE_{π}[d]	−245.4 (34.3)	−292.5 (49.2)	−228.5 (33.0) b_1: −143.8,[e] b_2: −84.7[e]	−50.0 (11.2)
Overlap σ	1.58	1.51	1.51	1.26
Overlap π	0.74	0.70	0.70	0.55
Bond length	1.10 (1.0977)	1.144 (1.1283)	1.144 (1.1283)	1.28 (1.2626)
ΔE (= −D$_e$)	−232.2	−258.4	−258.4	−180.8
D_o	228.8 (225.0)	255.4 (255.7)	255.4 (255.7)	278.9 (179.9)

[a]Energy values are given in kcal/mol. Bond lengths are given in Å. Experimental values are given in brackets. Data are taken from ref. 9.
[b]The symmetry is given by the electronic structure of the atoms with respect to the molecule, see Figure 6.
[c]Values in parentheses give the percentage of the total attractive interactions $\Delta E_{elstat} + \Delta E_{orb}$.
[d]Values in parentheses give the percentage of the total orbital interactions ΔE_{orb}.
[e]The b_1 value gives the electron-sharing contribution to the μ bond and the b_2 value gives the donor–acceptor contribution to the π bond, see Figure 6c.

planation for the stronger bond of CO in terms of ionic contributions is not supported by the calculations. The strength of the attractive covalent term for CO $\Delta E_{orb} = -594.2$ kcal/mol is also less than in N$_2$. The EDA data for CO(C$_{\infty v}$) indicate that carbon monoxide has a larger BDE than dinitrogen although the attractive forces in CO are weaker than in N$_2$. The higher bond energy of CO compared with N$_2$ comes from the weaker Pauli repulsion in the former molecule. The same conclusion becomes obvious from the EDA data for CO(C$_{2v}$) (Table 3). The Pauli repulsion in the latter arrangement is stronger ($\Delta E_{Pauli} = 725.9$ kcal/mol) than in CO(C$_{\infty v}$) ($\Delta E_{Pauli} = 575.8$ kcal/mol) but it is still weaker than in N$_2$ ($\Delta E_{Pauli} = 791.7$ kcal/mol). The attractive interactions in CO(C$_{2v}$) ($\Delta E_{elstat} = -291.1$ kcal/mol, $\Delta E_{orb} = -693.2$ kcal/mol) are weaker than in N$_2$. We want to emphasize, however, that the EDA results for the C$_{\infty v}$ approach of CO should be used for the interpretation of the chemical bond. The reason why CO has a stronger bond than N$_2$ is the significantly weaker Pauli repulsion in carbon monoxide.

The weaker Pauli repulsion in CO compared with N$_2$ can be explained in the same way as the weaker orbital interaction term because the strength of both terms, ΔE_{Pauli} and ΔE_{orb}, is mainly determined by the size of the overlap integral of the atomic orbitals. Table 3 shows that the σ and the π overlap in CO is smaller than in N$_2$. Note that the absolute values of ΔE_{Pauli} and ΔE_{orb} in the two molecules have the same magnitude.[†] The smaller orbital overlap in heteroatomic CO than in homoatomic N$_2$ means not only weaker covalent attraction in CO but also weaker Pauli repulsion. ΔE_{orb} becomes smaller in CO(C$_{\infty v}$) by 121.2 kcal/mol

but ΔE_{Pauli} is even reduced by 215.9 kcal/mol which more than compensates the loss of 68.5 kcal/mol electrostatic attraction. We want to point out that the EDA results for both arrangements of the atoms of CO indicate a substantial contribution of the π-bonding to the ΔE_{orb} term. In CO(C$_{\infty v}$), π-bonding is nearly as strong as σ-bonding (Table 3).

The arrangement of the atomic electronic structures in isoelectronic BF is straightforward (Fig. 6d). Similar as for CO, the EDA data show (Table 3) that the ΔE_{Pauli} term becomes smaller by 315.6 kcal/mol compared with N$_2$. However, the attractive interactions in BF are even 367.0 kcal/mol weaker than in N$_2$, because the ΔE_{elstat} value is reduced by 98.0 kcal/mol and the orbital interactions in BF are even 269.0 kcal/mol weaker than in N$_2$. The calculated BDE of BF ($D_e = 180.8$ kcal/mol) is therefore 51.4 kcal/mol smaller than the BDE of N$_2$. Is it possible to give a qualitative reason for the weaker bond energy of BF? Look at the σ and π contributions to the ΔE_{orb} term in CO and BF. The π contributions in CO are even larger than in N$_2$. It is interesting to note that π bonding in CO is nearly as strong as σ bonding. In BF, however, π bonding is rather weak. It contributes only 11.2% of the total covalent interactions while it provides 49.2% of the ΔE_{orb} term in CO(C$_{\infty v}$). The weaker π bonding in BF can not be explained with a weak overlap of the $p(\pi)$ AOs. Table 3 shows that the π overlap in BF (0.55) is not much smaller than in CO (0.70). Both components to the π bonding in BF arise from donor–acceptor interactions while the σ bond comes from electron-sharing interactions (Fig. 6d). The strength of the σ bond in BF ($\Delta E_{\sigma} = -396.4$ kcal/mol) is not much less than in N$_2$ and CO.

The EDA values suggest that the best Lewis structure for CO has a triple bond while the best Lewis structure for BF has a single bond. The EDA values also suggest that the weaker bond in BF compared with N$_2$ and CO is caused by the loss of π bond energy. The contribution of π bonding in BF to ΔE_{orb} (−50.0 kcal/mol) is 195.4 and 242.5 kcal/mol less than in N$_2$ and CO(C$_{\infty v}$), respec-

[†]This is not necessarily the case. Note that the attractive orbital interactions depend on the sign of the overlapping orbitals while the Pauli repulsion does not.
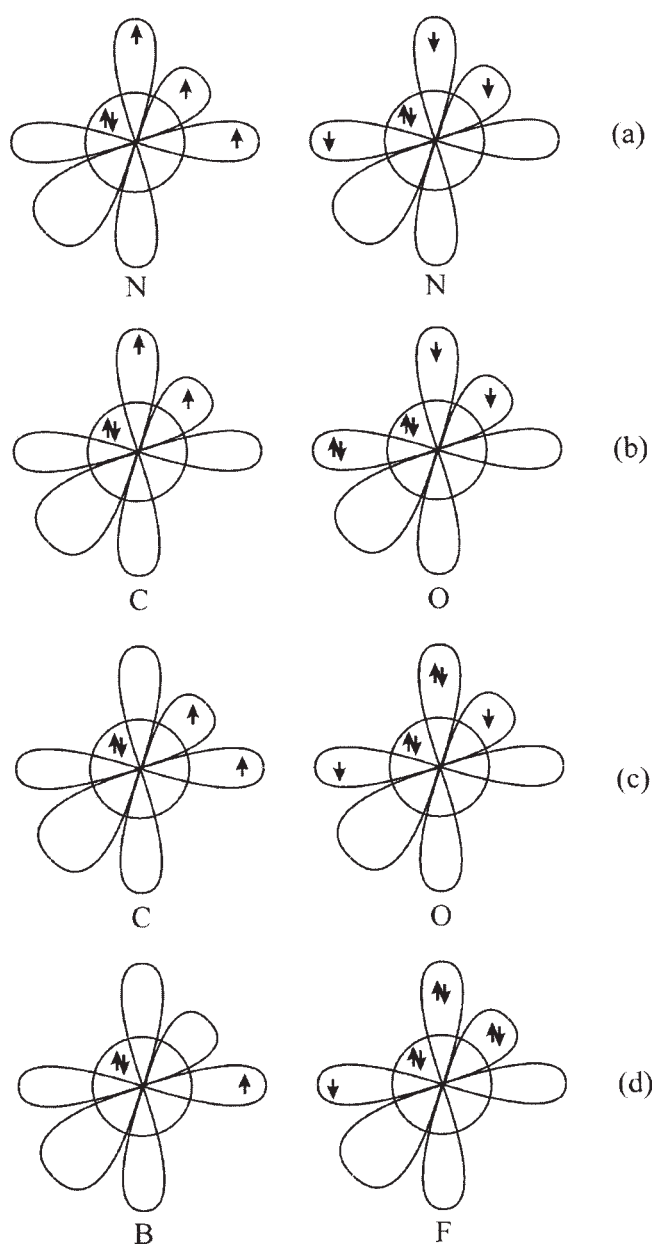
Figure 6. Schematic representation of the arrangement of the atomic electronic structures in the EDA calculations of N_2, CO and BF.

tively. If BF would have a π bond strength which is comparable to the latter diatomics it would have an even larger BDE than CO.

Conclusion

The development of modern quantum chemical methods for analyzing the electronic structure and bonding situation of molecules makes it possible to explain experimental observations with arguments that are based on well-defined mathematical definitions for partitioning the charge distribution or bonding energy into physically meaningful terms. The topological analysis of the electron density distribution shows nicely why CO is a C-nucleophilic agent although the carbon atom carries a positive partial charge. The 7σ HOMO of carbon monoxide plays a pivotal role for the chemical behavior and also for the dipole moment of the molecule. The 7σ HOMO of CO is not antibonding as it is often stated. The increase of the C—O bond strength after CO binds through its carbon atom to a σ acceptor such as H^+ is rather caused by the effect of the charge on the polarization of the bonding orbitals. The classical electrostatic attraction between carbon and oxygen and the covalent bonding are weaker than in N_2. The higher BDE of CO is caused by the much weaker Pauli repulsion. The π bonding contributions to the covalent interactions have nearly the same strength as σ bonding and they are stronger than in N_2. The reason for the lower BDE of BF compared with CO and N_2 comes from the much weaker π bonding contribution.

References

1. Huzinaga, S.; Miyoshi, E.; Sekiya, M. J Comput Chem 1993, 14, 1440.
2. Muenter, J. S. J Mol Spectrosc 1975, 55, 490.
3. Huber, K. P.; Herzberg, G. Molecular Spectra and Molecular Structure IV. Constants of Diatomic Molecules; Van Nostrand-Reinhold: New York, 1979.
4. Lupinetti, A. J.; Strauss, S. H.; Frenking, G. In Progress in Inorganic Chemistry, Vol. 49; Karlin, K. D., Ed.; Wiley: New York, 2001; p. 1.
5. (a) Willner, H.; Aubke, F. Organometallics 2003, 22, 3612; (b) Willner, H.; Aubke, F. Chem—Eur J 2003, 9, 1669.
6. (a) Goldman, A. S.; Krogh-Jespersen, K. J Am Chem Soc 1996, 118, 12159; (b) Lupinetti, A.; Fau, S.; Frenking, G.; Strauss, S. J. J Phys Chem A 1997, 101, 9551; (c) Lupinetti, A. J.; Jonas, V.; Thiel, W.; Strauss, S. H.; Frenking, G. Chem-Eur J 1999, 5, 2573; (d) Diefenbach, A.; Bickelhaupt, F. M.; Frenking, G. J Am Chem Soc 2000, 122, 6449.
7. (a) Bickelhaupt, F. M.; Radius, U.; Ehlers, A. W.; Hoffmann, R.; Baerends, E. J. New J Chem 1998, 22, 1; (b) Ehlers, A. W.; Baerends, E. J.; Bickelhaupt, F. M.; Radius, U. Chem—Eur J 1998, 4, 210; (c) Radius, U.; Bickelhaupt, F. M.; Ehlers, A. W.; Goldberg, N.; Hoffmann, R. Inorg Chem 1998, 37, 1080.
8. (a) Frenking, G.; Fröhlich, N. Chem Rev 2000, 100, 717; (b) Frenking, G. J Organomet Chem 2001, 635, 9; (c) Frenking, G.; Wichmann, K.; Fröhlich, N.; Loschen, C.; Lein, M.; Frunzke, J.; Rayón, V. M. Coord Chem Rev 2003, 55, 238.
9. Esterhuysen, C.; Frenking, G. Theoret Chem Acc 2004, 111, 381.
10. Bader, R. F. W. Atoms in Molecules. A Quantum Theory; Oxford University Press: Oxford, 1990.
11. (a) Fukui, K. Acc Chem Res 1971, 4, 57; (b) Fukui, K. Theory of Orientation and Stereoselection; Springer Verlag: Berlin, 1975; (c) Woodward, R. B.; Hoffmann, R. The Conservation of Orbital Symmetry; Verlag Chemie: Weinheim, 1970; (d) Fleming, I. Frontier Orbitals and Organic Chemical Reactions; Wiley: New York, 1976.
12. Ahsen, B. V.; Berkei, M.; Henkel, G.; Willner, H.; Aubke, F. J Am Chem Soc 2002, 124, 8371.
13. (a) Dewar, M. J. S. Bull Soc Chim Fr 1951, 18, C79; (b) Chatt, J.; Duncanson, L. A. J Chem Soc 1953, 2929.
14. Frenking, G. In Modern Coordination Chemistry: The Legacy of Joseph Chatt; Leigh, G. J.; Winterton, N., Eds.; The Royal Society: London, 2002; p. 111.
15. Ehlers, A. W.; Dapprich, S.; Vyboishchikov, S. F.; Frenking, G. Organometallics 1996, 15, 105.

16. (a) Woods, R. C. Philos Trans R Soc London Ser A 1988, 324, 141; (b) Berry, R. J.; Harmony, M. D. J Mol Spectrosc 1988, 128, 176 (Woods, R. C.; private communication).

17. (a) Albright, T. A.; Burdett, J. K.; Whangbo, M. H. Orbital Interactions in Chemistry; Wiley: New York, 1985; pp. 81, 82; (b) Elschenbroich, Ch.; Salzer, A. Organometallics, 2nd ed.; VCH: Weinheim, 1992; p. 227.

18. Lias, S. G.; Bartmess, J. E.; Liebman, J. F.; Holmes, J. L.; Levin, R. D.; Mallard, W. G. J Phys Chem Ref Data 1988, 17 (Suppl), 1.

19. Pauling, L. The Nature of the Chemical Bond, 3rd ed.; Cornell University Press: Ithaca, NY, 1960.

20. Pauling, L. General Chemistry; Dover: New York, 1970; p. 290.

21. (a) Morokuma, K. J Chem Phys 1971, 55, 1236; (b) Ziegler, T.; Rauk, A. Theor Chim Acta 1977, 46, 1.

22. (a) Bickelhaupt, F. M.; Baerends, E. J. In Reviews in Computational Chemistry, Vol. 15; Lipkowitz, K. B.; Boyd, D. B., Eds.; Wiley-VCH: New York, 2000; p. 1; (b) te Velde, G.; Bickelhaupt, F. M.; Baerends, E. J.; van Gisbergen, S. J. A.; Fonseca Guerra, C.; Snijders, J. G.; Ziegler, T. J Comput Chem 2001, 22, 931.

23. (a) Frenking, G.; Wichmann, K.; Fröhlich, N.; Loschen, C.; Lein, M.; Frunzke, J.; Rayón, V. M. Coord Chem Rev 2003, 55, 238; (b) Lein, M.; Frenking, G. In Theory and Applications of Computational Chemistry: The First 40 Years; Dykstra, C. D.; Kim, K. S.; Frenking, G.; Scuseria, G. E., Eds.; Elsevier: Amsterdam, 2005; p. 291.

24. Spackman, M. A.; Maslen, E. N. J Phys Chem 1986, 90, 2020.

25. Kovács, A.; Esterhuysen, C.; Frenking, G. Chem Eur J 2005, 11, 1813.